THE JOURNAL OF PHYSICAL CHEMISTRY B

 VOLUME 105, NUMBER 46, NOVEMBER 22, 2001

LETTERS

Single Nanowire Lasers

Justin C. Johnson, Haoquan Yan, Richard D. Schaller, Louis H. Haber, Richard J. Saykally,*,† and Peidong Yang*,‡

Department of Chemistry, University of California, Berkeley, California 94720-1460

Received: June 19, 2001; In Final Form: August 23, 2001

Ultraviolet lasing from single zinc oxide nanowires is demonstrated at room temperature. Near-field optical microscopy images quantify the localization and the divergence of the laser beam. The linewidths, wavelengths, and power dependence of the nanowire emission characterize the nanowire as an active optical cavity. These individual nanolasers could serve as miniaturized light sources for microanalysis, information storage, and optical computing.

Introduction

Light-emitting nanostructures are of much current interest due to their unique physical properties and their potential applications, including optoelectronic devices and microanalysis.[1−3] The recent observation of bulk lasing from epitaxially grown zinc oxide (ZnO) nanowire arrays[4] represents a significant advance toward producing intense nanoscale sources of coherent light. Characterization of the lasing action from single wires and its dependence on the morphology of the wire can be facilitated by high-resolution near-field optical imaging and spatially resolved spectroscopy.[5−7] Here we describe the first observation of single ZnO nanowires acting as both optical waveguides and lasers, depending on the quality factor of the cavity of the wire. Near-field images and spatially resolved photoluminescence (PL) spectra reveal the localization of the laser field in the vicinity of the wire and the properties of the beam as it diverges from the sub-wavelength source. The linewidths and wavelengths of the laser radiation characterize the nanowire as an active optical cavity.

Zinc oxide is a wide band-gap (3.37 eV, 298 K) semiconductor that recently has been shown to exhibit photoluminescence gain and random lasing in thin films and microstructures.[8−10] However, the threshold for lasing in such structures has been high (∼300 kW/cm^2), primarily due to the high carrier concentration required for the electron−hole plasma lasing mechanism. Low-dimensional nanostructures facilitate lasing by excitonic recombination since the density of states near the band gap edges is enhanced in such structures. The large ZnO exciton binding energy (60 meV) further facilitates this gain mechanism, even at room temperature. Lasing from ZnO nanowires has been observed by exciting a collection of densely packed wires on the growth substrate,[4] but no information about the laser emission from single wires has ever been obtained.

Experimental Section

The ZnO nanowires used in this study were grown vertically on a sapphire substrate using the methods described in refs 4 and 11. Briefly, the wires were synthesized using a vapor phase transport process, with an Au thin film catalyzing the epitaxial crystal growth. The ZnO wires grow preferentially on the (110) plane of sapphire, which makes a good epitaxial interface with the (0001) plane of ZnO. A scanning electron microscopy (SEM) image of the densely packed wires grown on sapphire is shown in Figure 1a, along with an end-view image of the nanowires (Figure 1b). The diameters of the wires vary between 40 and 150 nm, and their lengths can be controlled to be between 4 and 10 μm. The hexagonal end faces seen in the end-view SEM

* To whom correspondence should be addressed.
† E-mail: saykally@uclink4.berkeley.edu.
‡ E-mail: pyang@cchem.berkeley.edu.

10.1021/jp012304t CCC: $20.00
Published on Web 10/23/2001

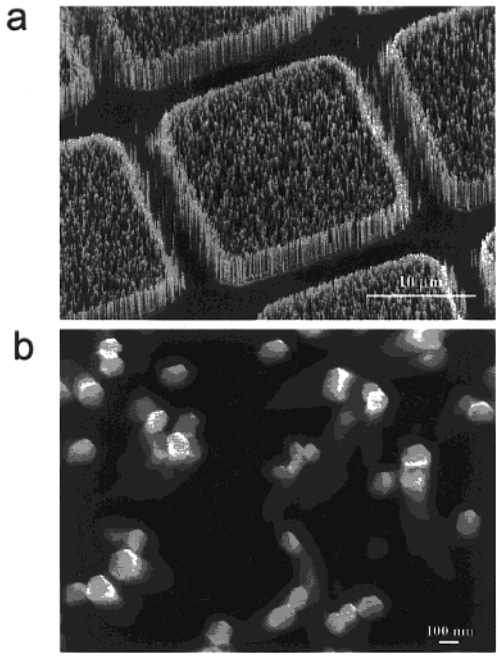

Figure 1. Scanning electron microscopy images of zinc oxide nanowires. (a) Wires grown vertically on a sapphire substrate. (b) End-view SEM image of the nanowires showing the well-defined hexagonal end planes.

image serve as mirror planes for the laser cavities. To be imaged with the near-field scanning optical microscope (NSOM), the wires were removed from the sapphire growth substrate by sonication and dispersed onto a quartz substrate by drop casting an ethanol-nanowire mixture. This procedure produced free-standing horizontal wires with a density of about 10^3 wires per mm^2.

The nanowires were excited with short pulses (<1 ps) of 4.35 eV photons (285 nm) in order to induce photoluminescence (PL) and lasing. The pulses were generated by frequency-doubling the sum frequency of a tunable near-IR pulse and an amplified 800 nm pulse from a mode-locked Ti:sapphire oscillator. The UV beam was spatially filtered using prisms and was directed to the sample at an angle of approximately 45°. The beam was focused to a spot diameter of approximately 200 μm. The nanowire emission was collected by a chemically etched[12] fiber optic probe held in constant-gap mode by the feedback electronics of the NSOM.[13] The NSOM collected topographic (corresponding with the shear-force feedback signal) and optical information simultaneously on both forward and reverse scans (100 pixels × 100 pixels each), which were added to reduce background noise.

Results and Discussion

Figure 2 shows a topographic (a) and an NSOM PL (b) image of a single nanowire. The wire in the topographical image has a length of 5 μm and a diameter of about 140 nm, as determined by the height of the wire on the substrate. The corresponding optical image in Figure 2b shows the spatially resolved emission collected in a 70 nm wide spectral band centered at 400 nm. Strong PL emission at the end of the nanowire can be clearly seen in Figure 2b, while only very weak emission was detected from the side surfaces of the nanowire. The PL spectrum collected at the nanowire end (Figure 2**c**), corresponds well with the broad ZnO spontaneous emission. The enhanced intensity at the ends of the wire indicates increased scattering of the PL

Figure 2. Near-field images of a single ZnO nanowire waveguide. (a) Topographical and (b) PL NSOM image size is (10 μm),[2] with maximum topographical height of 140 nm. The sample was excited with approximately 100 nJ pulses at 285 nm, resulting in an excitation intensity of about 200 kW/cm^2. (c) The PL spectrum from the wire (fwhm ≈ 20 nm), which did not show narrowing upon increasing the excitation intensity.

photons as they reach the end of the waveguide. However, there was no apparent lasing from the wire even at very high peak excitation intensities (>1 MW/cm^2). This waveguide behavior was observed for several cleaved wires of similar dimension, and the absence of lasing suggests that many of the wires are not suitable cavities to support sustained optical gain. This can be ascribed to the way in which we disperse the nanowires on the substrate. The current procedure inevitably fractures the wires from the sapphire in a fashion that is likely to decrease the quality factor of the cavity of the wire by forming less well-defined end planes. In addition, cavity losses may result from the wire contacting the quartz substrate, which has a refractive index of 1.6, compared with 2.45 for ZnO. Thus, it is not surprising that the fraction of dispersed wires that exhibit lasing will decrease markedly from that found for wires attached to the growth substrate.

Shown in Figure 3 is a combined topographical and optical image of a nanowire that appears to remain attached to a piece

Figure 3. Near-field image of a ZnO nanowire laser. (a) Combined topographical and NSOM image size is $(14\mu m)^2$. The maximum topographical height on the wire is 200 nm. The excitation intensity is about 150 kW/cm^2. Overall signal contrast is about 10:1 from the bright portions of the image to the regions that exhibited no lasing. Small topographic features at the top and left side of the images showed high signal, apparently due to scattering of the nanowire laser radiation. The small feature at the bottom of the image blocks the laser radiation as it emanates from the end face of the wire. The same region exhibited little contrast with lower intensity excitation. (b) Emission spectra (slightly offset for clarity) from the positions labeled by the numbers on the image (a).

of fractured sapphire substrate. The wire has a length of 6−7 μm and a topographical height of 200 nm, indicating that it is possibly elevated above the quartz substrate. The optical image (given by the color scale) in Figure 3a shows a remarkable increase in signal with the probe directly above and within several microns of the large wire, as well as a cone of weaker signal emanating from the end of the wire. The approximate divergence angle[14] of the nanolaser beam is 70 degrees (assuming the near-field probe samples a slice of the three-dimensional beam cone), implying a diffraction-limited source size of 200 nm, which corresponds fairly well with the observed topographical diameter of the wire.

Significant peak narrowing is observed for the emission emanating from the end of the nanowire versus that collected directly above the wire. Spectrum 1 shown in Figure 3b is taken from the brightest region (area 1 in Figure 3a) and exhibits two clear lasing peaks at 380.8 and 384.0 nm. Spectrum 2 in Figure 3a is taken from the cone below the wire (area 2) and shows one lasing peak but an integrated spectral intensity approximately five times lower than on the wire. The dark areas of the image did not exhibit lasing. The wire fragment in the lower portion of Figure 3a appears to block the laser beam as it emanates from the wire, resulting in a dark streak in the laser cone. The fact that this wire laser appears to have its end faces undamaged from sample preparation indicates that maintaining high quality cavity end faces is crucial for the wires to support lasing. The lack of unambiguous lasing from other fractured wires lying on the substrate affirms this idea, though the possibility exists that substrate effects also perturb the nanowire cavity and inhibit lasing.

Figure 4. Lasing and PL images of a nanowire with limited substrate contact. (a) Combined topographic and NSOM image with approximately 200 kW/cm^2 intensity excitation. (b) Optical image of the same region as in a, with 150 kW/cm^2 excitation. (c) PL image (exhibiting little contrast) taken with collection of a spectral band centered away from the lasing peak (377 nm). (d) Typical spectrum from images a and b, showing the spectral bands that were collected in the optical images. The image size is $(16\ \mu m)^2$, and the nanowire has a diameter of approximately 200 nm (taken from the lowest height of the nanowire from the substrate). The apparent broadening of the upper end of the wire is primarily a topographical artifact due to its being raised above the substrate by a smaller nanowire situated underneath it.

Lasing was also observed from a nanowire that was situated at an angle to the quartz substrate, shown in Figure 4. The images in Figure 4a,b are the result of collecting a narrow spectral band (<3 nm) centered at 380 nm (see Figure 4d), while the image in Figure 4c maps a 3 nm spectral band centered at 377 nm, at which no lasing occurred. The intense signal collected near the ends of the nanowire in Figures 4a,b demonstrates the confinement of the nanowire lasing emission to a cone-shaped region near the end faces. The fact that the wire appears to have only one point of contact with the quartz substrate further supports the conclusion that large areas of nanowire-substrate contact increase cavity losses in the wire. The clear lasing behavior demonstrated in Figures 3 and 4 was observed for only a few (out of several hundred) nanowires studied and was not seen in fractured wires or wires lying horizontally on the substrate.

The power dependence of the nanowire emission, shown in Figure 5a, exhibits a clear threshold near excitation intensity of approximately 120 kW/cm^2 (using a subpicosecond laser pulse width). This threshold is higher than that observed from bulk wires, though it is the same order of magnitude. The single nanolasers dispersed onto the quartz substrate are likely to exhibit a higher threshold than those attached to the growth substrate, considering the possible damage to the end faces that occurs during sample preparation. Nanowire coupling could also contribute to the lower lasing threshold observed for the nanowire arrays.[4]

The spectral width of the laser peak measured directly above the wire is about 3.0 nm (Figure 3a, area 1), which is quite

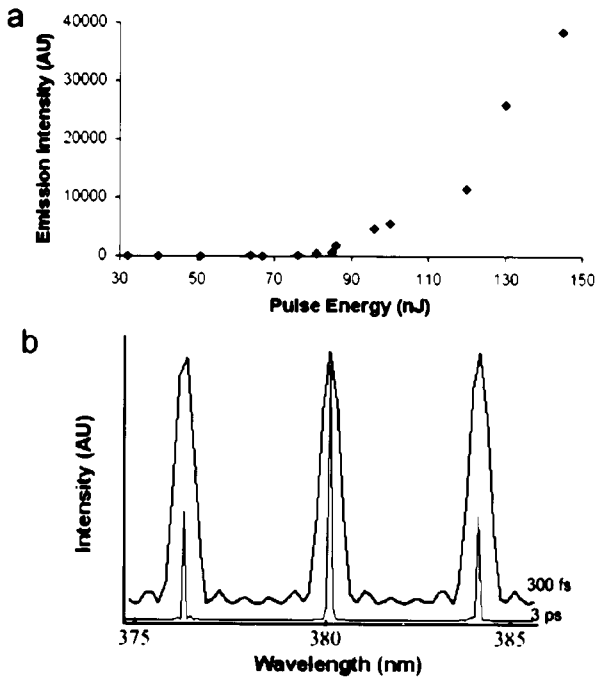

Figure 5. (a) Power dependence of the emission signal as a function of excitation intensity. Laser spot diameter was approximately 0.5 mm. (b) Simulated spectra for a ZnO cavity of 6.85 μm in length supporting a single transverse cavity mode. The upper trace shows the total field intensity after 3 full passes (300 fs) through the cavity. The lower spectrum was calculated for 30 passes (3 ps). The spectra were obtained by calculating the intensity of the interfering fields in the cavity at each wavelength. The simulation does not account for gain within the cavity.[15]

broad compared to previously observed ZnO lasing (<0.3 nm) and compared to the peak observed in the spectrum measured off the wire (width $\approx$ 1.2 nm, Figure 3a, area 2). This is also much wider than the instrumental spectral resolution (<0.4 nm), suggesting that the spectrum collected from above the wire originates from both lasing modes and nonlasing PL that is not sustained in the cavity, either because its direction of propagation is nonaxial or because its wavelength does not correspond with one of the longitudinal cavity modes. Laser intensity along the wire axis, but far from the nanowire, is only strong if the photons are directed by the cavity, thus it is expected that the linewidth of that emission would be narrower. Another factor that could contribute to peak broadening is the low reflectivity of the nanowire end faces (18%, based on Fresnel equations), which leads to short average cavity confinement times. Thus, many modes that are poorly supported in the cavity can experience gain during the excitation pulse period but do not completely destructively interfere in only a few passes through the wire (three reflections produce >99% transmission losses). Therefore, the overall cavity confinement time is likely to be approximately equal to the excitation lifetime, since this is the only period in which the optical gain (associated with stimulated emission) will be able to counteract reflection losses. A simulation of this behavior for a nanowire cavity is shown in Figure 5b, which demonstrates the peak narrowing that occurs for longer cavity confinement times. The simulation for photons taking three full passes through the cavity (about 300 fs) produced a linewidth of about 1.0 nm, which corresponds well with the observed lasing linewidth in the nanolaser beam.

Future study of excitation wavelength, pulse width, quality factor, and substrate effects should lead to a more complete description of the physical properties of these single nanowire lasers, which will direct efforts toward engineering these nanostructures for use in practical devices.

Acknowledgment. P.Y. and H.Y. are supported in part by a New Faculty Award from Dreyfus Foundation, a Career Award from the National Science Foundation, Research Corporation, Department of Energy and start-up funds from the University of California, Berkeley. P.Y. is an Alfred P. Sloan Research Fellow. P.Y. thanks the 3M company for an untenured faculty award. We thank the National Center for Electron Microscopy for the use of their facilities. R.J.S., R.D.S, L.H., and J.C.J are supported by the Physical Sciences Division of the National Science Foundation. We thank P. Peterson and K. Knutsen for useful discussions and assistance in data collection.

References and Notes

(1) Duan, X. F.; Huang, Y.; Cui, Y.; Wang, J.; Lieber, C. M. *Nature* **2001**, *409*, 66.

(2) Klimov, V. I.; Mikhailovsky, A. A.; Xu, S.; Malko, A.; Hollingsworth, J. A.; Leatherdale, C. A.; Eisler, H.-J.; Bawendi, M. G. *Science* **2000**, *290*, 314.

(3) Pavesi, L.; Negro, L. D.; Mazzoleni, C.; Franzo, G.; Priole, F. *Nature* **2000**, *408*, 440.

(4) Huang, M. H.; Mao, S.; Feick, H.; Yan, H.; Wu, Y.; Kind, H.; Weber, E.; Russo, R.; Yang, P. *Science* **2001**, *292*, 1897.

(5) Nguyen, T., Schwartz, B. Schaller, R. D., Johnson, J. C., Lee, L. F. Haber, L. H.; Saykally, R. J. *J. Phys. Chem. B* **2001,** *105*, 5153.

(6) Baba, T.; Yamada, H.; Sakai, A. *Appl. Phys. Lett* **2000**, *77*, 1584.

(7) Buratto, S. K.; Hsu, J. W. P.; Trautman, J. K.; Betzig, E.; Bylsma, R. B.; Bahr, C. C.; Cardillo, M. J. *J. Appl. Phys.* **1994**, *76*, 7720.

(8) Yu, P.; Tang, Z. K.; Wong, G. K. L.; Kawasaki, M.; Ohtomo, A.; Koinuma, H.; Segawa, Y. *J. Cryst. Growth.* **1998**, *184/185*, 601.

(9) Bagnall, D. M.; Chen, Y. F.; Zhu, Z.; Yao, T.; Koyama, S.; Shen, M. Y.; Goto, T. *Appl. Phys. Lett*. **2000**, *70*, 2230.

(10) Cao, H.; Xu, Y. Y.; Zhang, D. Z.; Chang, S.-H.; Ho, S. T.; Seelig, E. W.; Liu, X.; Chang, R. P. H. *Phys. Rev. Lett.* **2000**, *84*, 5584.

(11) Huang, M. H.; Wu, Y.; Feick, H.; Tran, N.; Weber, E.; Yang, P. *Adv. Mater.* **2001,** *13*, 113.

(12) Nishiwaya, S. M.; Isu, T. *J. Microsc.* **1999**, *194*, 415.

(13) Ruiter, A. G. T.; Van Der Werf, K. O.; Veerman, J. A.; Garcia-Parajo, M. F.; Rensen, W. H. J.; Van Hulst, H. F. *Ultramicroscopy* **1998**, *78,* 149.

(14) Guenther, R. *Modern Optics*; Wiley: New York, 1990; p 341.

(15) A quantitatively accurate value for the gain coefficient of a single ZnO wire is difficult to obtain under the current experimental conditions, though efforts are ongoing to measure such a value. Gain coefficients for ZnO thin film lasing are of the order 280 cm^{-1}, with gain thresholds slightly higher than those observed here.[8] Thus, with the shorter optical cavity length of the nanowires versus thin films and similar lasing and loss mechanisms, it is expected that the gain coefficient of the observed lasing nanowires is comparable to 280 cm^{-1}.